Transient Response of Multiquantum Well Vertical-Cavity Surface Emitting Lasers

Raad S. Fyath, Saad M. Falh, and Fadil R. Tahir
University of Basra, Collage of engineering, Electrical engineering Department

Abstract

The dynamic performance of vertical-cavity surface emitting lasers (VCSEL) diodes can be enhanced by incorporating multiquantum-well (MQW) structure in the active region. This paper addresses the transient response of MQW-VCSEL by solving the laser rate equation in the large-signal regime. The analysis makes use of the energy band structure and optical gain spectrum obtained by applying Schrödinger equation to both conduction and valance bands. Simulation results are presented for 1.3 μm InGaAs/InP VCSEL and indicate clearly that a MQW laser has higher switching speed compared with bulk laser and this finding is more pronounced with small number of wells.

الاستجابة العابرة لليزرات الانبعاث السطحي ذات الفجوة العمودية-متعددة الآبار الكمية

رعد سامي فياض- سعد محي فالح- فاضل رحمة طاهر
(جامعة البصرة,كلية الهندسة, قسم الهندسة الكهربائية)

الخلاصة

أن أداء ليزرات الانبعاث السطحي بالإمكان تحسينه باستعمال متعدد الآبار الكمية (MQW) في المنطقة الفعالة له, في هذا البحث نقدم تحليل للاستجابة العابرة لهذا النوع من الليزرات من خلال حل معادلات التغير الزمني (Rate equations) لها في طور الإشارة الكبيرة (large signal) . الدراسة تضمنت استعمال معادلة شرودينكر (Schrödinger equation) لحساب تركيب حزم الطاقة (Energy band structure) و طيف الكسب الضوئي (Optical gain spectrum) . نتائج المحاكاة (Simulation) للتركيب (InGaAs/InP) الذي يعمل بطول موجي (1.3μm) عرضت في هذا البحث والتي بينت بوضوح بأن الليزرات ذوات المنطقة الفعالة متعددة الآبار الكمية تملك سرعة اقلاب (Switching speed) عالية مقارنة مع الليزرات التقليدية, وهذه النتيجة تكون اكثر وضوحا كلما قل عدد الآبار الكمية في المنطقة الفعالة.

1-introduction

In the recent years, vertical-cavity surface emitting lasers (VCSELs) are playing key roles for various applications including optical computing, optical data processing, and optical switching networking. They can be implemented in two-dimensional (2D) emitter arrays and designed for single-mode operation [1-4].

A conventional injection semiconductor laser consists of two cleaved end mirrors perpendicular to the active region so that only one-dimensional laser arrays can be monolithically fabricated. The built-in resonator used in a VCSEL is normally formed by two surface of an epitaxial layer and the light output is taken vertically from the top of the surface rather than the end facets [5], [see Fig.1]. Moreover, their vertical geometry supports easy integration in high performance 2D laser arrays. The VCSEL provides many advantages such as [6-8]; (i) ultra low threshold current is achieved by introducing the microcavity structure, (ii) dynamic-single mode operation is expected because of large longitudinal mode spacing, (iii) a sharp circular beam can be obtained due to their circular emitting area, and (iv) monolithic integration with other devices is feasible. For example, surface normal optical switches based on VCSELs represent a promising 2D approach to high-throughput optical data processing [9].

To enhance the performance of VCSELs further, the active region may be fabricated using multiquantum well (MQW) structure. This structure contains alternating thin layers of a narrow-bandgab material (well) and a wide-bandgap material (barrier). The thickness of the well region is chosen to be less than the carrier wavelength (deBroglie wavelength) to enhance the effect of quantum mechanics. Conventional and VCSELs containing MQW active region have shown less threshold current and less temperature sensitivity when compared with bulk counter parts [10].

In this paper, we investigate theoretically the dynamic response of the (InGaAs/InP) MQW-VCSEL in the large-signal regime. In section II, a theoretical scheme is presented for evaluating the gain spectra and spontaneous emission rate using conduction and valence band energy structure. In section III, the single-longitudinal spatial mode rate equations have been formulated and solved numerically to study the transient response of MQW-VCSEL. In section IV, simulation results on optical gain spectra and large-signal response of the laser are discussed in detail. Also, this section is devoted to examine the effect of laser parameters (facet reflectivity and number of wells) on switching time and over shoot power. Final a summery is presented in section V.

II-Theory

A. MQW-structure:

The MQW laser under study contains $In_{0.53}Ga_{0.47}As$ well layer of thickness W_z and InP barrier layer of thickness W_b, as shown in Fig. (1b). All layers comprising the guiding layer are assumed to be undoped with total thickness of L_t. The optical confinement region is embedded in n- and p-InP cladding layers. By applying a suitable forward bias voltage to the laser, nearly flat-band conditions exist in the active region as depicted in Fig. (1), and large current flows through the layers. Certain electrons and holes are confined to the well regions with discrete levels (E_{cn}, E_{Hm}, and E_{Lm}, n and m= integers). The subscript c, H, and L denote, respectively, conduction band, heavy-hole valance band, and light-hole valance band.

B. Evaluation of energy subband structures:

It is well known that for a MQW system, if the barrier thickness is thick enough, each single well can be treated as n isolated well [11]. The evaluation of the electronic states of the quantum well is based upon the envelope function approximation [12]. Quantum confinement

of carriers splits the conduction and the valence bands of the bulk material into a number of subbands. The energy of these subbands are equal to the energy levels in the one dimensional potential well defined by the line up of the band edge in the two component materials.

The wave function and quantized energy levels are calculated by solving Schrodinger equation for both conduction and valence bands. For the conduction band this equation reads [13],

$$\left[-\frac{\hbar^2}{2m_c}\cdot\frac{\partial^2}{\partial z^2}+V(z)\right]\cdot\Phi_{cn}(z) = E_{cn}\Phi_{cn}(z) \qquad (1)$$

where $\hbar = 2\cdot\pi\cdot\hbar$ is Planck constant, $\Phi_{cn}(z)$ is the envelope function, m_c is the effective mass, V(z) is the potential well, and E_{cn} is the quantized energy levels to be calculated.

The origin of the energy in the conduction band is taken at the bottom of the conduction band well. $\Phi_{cn}(z)$ is obtained from eqn. 1 as,

$$\Phi_{cn}(z)=\begin{cases} A\begin{bmatrix}\cos\\ \sin\end{bmatrix}\left[\frac{\sqrt{2m_cE_{cn}}}{2\hbar}\cdot z\right] & \begin{bmatrix}n:even\\ n:odd\end{bmatrix}\ |z|\le\frac{W_z}{2} \\ B\cdot\exp\left[-\frac{\sqrt{2m_{c1}(\Delta E_c-E_{cn})}}{\hbar}\cdot|z|\right] & |z|>\frac{W_z}{2}\end{cases} \qquad (2a)$$

where A and B are constants. In eqn. 2a, the effective mass is distinguished between the well and the barrier as m_c and m_{c1} ,respectively. Since $\Phi_{cn}(z)$ and it's derivative are continuous at the heterointerface, E_{cn} is obtained from the above equation as discrete value

$$\left[\frac{m_{c1}}{m_c}\cdot\frac{\Delta E_c-E_{cn}}{E_{cn}}\right]^{0.5} = a\cdot\tan^a\frac{W_z\sqrt{2m_cE_{cn}}}{\hbar} \qquad (2b)$$

where $a=(-1)^n$, n=0, ,1, 2, ...

Since electrons are free for the directions parallel to the hetrojunction, the total energy of an electron ε_{cn} is given by:

$$\varepsilon_{cn} = E_{cn} + \frac{\hbar^2k^2}{2m_c} \qquad (2c)$$

where k is the wave vector parallel to the interface of the hetrojunction. Similar calculations are also applied to the heavy hole and light hole valence band.

C-Gain and spontaneous emission spectra

One of the most efficient theories to calculate the optical gain is the density matrix theory based on the relaxation broadening model [14]. Using this theory and under nearly flat-band conditions, one can get a good approximate model to describe the optical gain in the laser cavity. Let assume an electron in the n^{th} state in the conduction band with energy ε_{cn} and the state is occupied with a probability of F_c at a quasi-Fermi level E_{fc}. In the other hand, there is a hole in the m^{th} state in the valance band with energy ε_{hm}, where h=H for heavy hole and h=L for light hole. This state is occupied with probability of F_h at quasi-Fermi level E_{fv}. For conservation of momentum in the x-y plan, one must have $k_c=k_h=k$. When an electron recombines with either a heavy hole or light hole, a photon polarized in a p-direction with an energy E_{ph} is emitted in the z direction. The probability of transition from n^{th} state of electron to the m^{th} state of the hole is equal to $\left\langle R_{ch}^2\right\rangle_{nm}$.

Since the potential wells in the conduction and valence bands have the same symmetry with each other, one can

write the probability of transition from n^{th} state of electron to the m^{th} state of hole as equal to $\left\langle R_{ch}^2 \right\rangle \cdot \delta(n-m)$, where $\delta(n-m)$ is Dirac delta function. The optical gain can be written as [14]:

$$g(E_{ph}) = \frac{E_{ph}}{\hbar\sqrt{\varepsilon_o \cdot \mu_a}} \sum_{h=H,L} \sum_{n=0}^{M-1} \int_{E_{gn}}^{\infty} \xi \, dE_{cn} \quad (3)$$

with

$$\xi = \left\langle R_{ch}^2 \right\rangle \frac{D_{ch}(F_c - F_v)(\hbar/\tau_{in})}{(E_{cn} - E_{ph})^2 + (\hbar/\tau_{in})^2} \quad (4a)$$

$$\left\langle R_{ch}^2 \right\rangle = \frac{1}{2}|R_h|^2 \cdot (1 + \frac{E_{cn}}{E_{ch}}) \quad (4b)$$

$$|R_{ch}| = \frac{q^2\hbar^2}{4E_{ch}^2 m_c}(\frac{m_o}{m_c} - 1)(\frac{E_g(E_g + \Delta)}{E_g + \frac{2\Delta}{3}}) \quad (4c)$$

$$D_{ch} = \frac{m_r}{\pi\hbar W_z}, \quad m_r = \frac{m_c m_h}{m_c + m_h} \quad (4d)$$

$$F_c = \frac{1}{1 + \exp(\frac{\varepsilon_{ch} - E_{fc}}{K_B T})} \quad (4e)$$

$$F_v = \frac{1}{1 + \exp(\frac{\varepsilon_{hn} - E_{fv}}{K_B T})} \quad (4f)$$

where

E_{cn} = Transition energy

μ_a = Refractive index of the well material

ε_o = Permittvity of the vacuum

M = Number of subbands

τ_{in} = Intraband electron relaxation time

m_o = Mass of the free electron

m_h = Effective mass of hole

K_B = Boltzman constant

T = Operating absolute temperature

Δ = Spin-orbit splitting

q = Electron charge

Forther, E_{gn} is related to the band gap energy of the well material E_g by:

$$E_{gn} = E_{cn} + E_{hn} + E_g \quad (4g)$$

The expression of the spontaneous emission can be determined by replacing $(F_c\text{-}F_v)$ and $\left\langle R_{ch}^2 \right\rangle$ in eqn. 3 by $F_c(1\text{-}F_v)$ and $\left\langle R_{ch}^2 \right\rangle_{avg}$, respectively. Using the average square of the matrix element $\left\langle R_{ch}^2 \right\rangle_{avg}$ rather than $\left\langle R_{ch}^2 \right\rangle$ is justified since the spontaneous emission is unpolarised. Therefore, $\left\langle R_{ch}^2 \right\rangle_{avg}$ is computed by averaging the momentum matrix over all directions [15].

$$r_{sp}(E_{ph}) = \frac{E_{ph}}{\hbar\sqrt{\varepsilon_o \cdot \mu_a}} \sum_{h=H,L} \sum_{n=0}^{M-1} \int_{E_{gn}}^{\infty} \Psi \cdot dE_{ch} \quad (5)$$

with

$$\Psi = \left\langle R_{ch}^2 \right\rangle_{avg} \frac{D_{ch} F_c (1 - F_v)(\hbar/\tau_{in})}{(E_{cn} - E_{ph})^2 + (\hbar/\tau_{in})^2} \quad (6a)$$

$$\left\langle R_{ch}^2 \right\rangle_{avg} = \frac{q^2\hbar^2}{6m_o E_{ph}^2}(\frac{m_o}{m_c} - 1) \cdot (\frac{E_g(E_g + \Delta)}{E_g + \frac{2\Delta}{3}}) \quad (6b)$$

Recall that g in eqn. 3 and r_{sp} in eqn. 5 are calculated for an isolated well. For a MQW laser with N_w wells, the system has gain spectrum of $N_w g$ and a spontaneous emission rate spectrum of $N_w r_{sp}$. Thes spectra may have multiple peaks located.

$$E_{ph} = E_{cn} + E_{hm} + E_g = h\nu_{nm} \quad (7)$$

where ν_{nm} is the emitted light frequency for the optical transition from the n^{th} state (electron) to the m^{th} state (hole).

III-Rate equations

Figure (1a) shows a simplified structure of a 1.3 μm InGaAS/InP quantum well active region VCSEL that is used in this study. The introducing of InGaAs wells in InP material and employing high reflectivity multilayer mirrors allow an ultralow threshold operating condition. Consider a uniform distribution of average photon population S(t) and injection carrier population N(t) in the cavity. Assume further that the carriers are completely confined in the wells while the photons are partially confined there. These assumptions are always justified in MQW semiconductor laser [1]. The rate equation for a MQW-VCSEL operating with a single longitudinal spatial mode can be developed by adopting the rate equation of a conventional(bulk)semiconductor laser[16]. The developed equations take into the account the structure parameters of the MQW - VCSELs. The results are:

$$\frac{dN}{dt}=\frac{I}{q}-\frac{\Gamma V_g g(E_{ph})}{1+\frac{\Gamma\varepsilon S}{V}}S - [A_{nr}+C(\frac{N}{V})^2]N - R_{sp} \quad (8a)$$

$$\frac{dS}{dt}=\frac{\Gamma V_g g(E_{ph})}{1+\frac{\Gamma\varepsilon S}{V}}S - V_g\gamma S + \Gamma\beta R_{sp} \quad (8b)$$

with

$$\Gamma = N_w\Gamma_w \quad (9a)$$

$$\Gamma_w=\frac{W_z}{L_t} \quad (9b)$$

$$L_t = N_w W_z + (N_w-1)W_b + 2W_c + 2W_m \quad (9c)$$

$$R_{sp}=\int\frac{\mu_a^3\varpi^2}{\pi^2\hbar c^3}r_{sp}(\hbar\varpi)d\varpi \quad for\ all\ \varpi \quad (9d)$$

$$\gamma=\Gamma\gamma_{ac}+(1-\Gamma)\gamma_{ex}+\gamma_m \quad (9e)$$

$$\gamma_m=\frac{1}{L_t}\ln\left(1/\sqrt{R_t R_b}\right) \quad (9f)$$

$$\beta=\frac{3}{2}\cdot\frac{\lambda^4}{4\pi^2\mu_a^2\mu_g\Delta\lambda_{sp}V^2} \quad (9g)$$

The symbols used in the rate equations are defined in Table I.

In the VCSEL, the optical wave is traveling in an isotropic region containing many different layers with various doping concentrations and penetrates a finite length into the mirror region where further scattering losses, diffraction losses, and absorption losses, may occurs [7]. Approximately, we can write the total length of the cavity as an effective length equals to the physical of the cavity plus penetration depth, W_m, into the top and bottom mirrors. Therefor, L_t is used as an effective cavity length.

The output power emitted from each facet is related linearly to the photon population and it is given by [16].

$$P_o=\frac{1}{2}\hbar\varpi V_g\gamma_m S \quad (10)$$

The term $V_g\gamma_m$ is the rate at which photons of energy $\hbar\varpi$ escape through the two facets, with V_g is group velocity and γ_m is the mirror losses.

IV-Results and Discussions

In this section, simulation results are presented for $In_{0.53}Ga_{0.47}As/InP$ using the parameter values listed in Table II.

The subbands energy are calculated by solving the Schrödinger equation. Table III shows a detailed structure of the energy subbands and their populations when the carrier density N = $3*10^{18}cm^{-3}$, (the populations are presented in a normalized form with respect to $3x10^{18}$ cm^{-3}).

The effect of intraband relaxation on the gain spectra of the laser is shown in Fig. 2. The solid line corresponding to τ_{in}=0.1 psec. and the dashed line corresponds to $\tau_{in}\to\infty$, the ideal case. Notice that the effect of intraband

relaxation in MQW structure is large compared to bulk structure.

The dependence at optical gain on carrier density is shown in Fig. 3. The main features of this figure are:

1. When N is small, the gain spectrum is narrow and the gain peak occurs at the first subband edge.
2. As N increases, the gain at first subband increases rabidly until the states in the first subband is filled perfectly by the carriers. Now, if N increases further they carrier population in the first subband remains constants and therefor the gain dose not change. In the other hand, the gain at the second subband starts to increase and the maximum gain shifted from the first subband to the second subband. This means that the lasing frequency change from the first frequency corresponding to the first subband to the other frequency corresponding to the second subband.

The characteristics of MQW-VCSEL during switching transients are then studied. The results obtained for these advanced lasers are compared with those simulated for a bulk-VCSEL. The parameters value for a bulk laser are identical to those adopted for MQW laser except the peak gain coefficient is assumed to have linear dependence on carrier density. The temporal evaluation of N and S are obtained by solving the single-mode rate equations.

The laser current is abruptly increased, say when time t=0, from its initial value I_0 to the final value I_f, which is greater than threshold current I_{th}. The following results are obtained with I_o=0 while I_f is set up to the level required to yield an output power P_o=3mW per facet. Figure (4a) shows the transient response of the electron population N and the output power P_o for the MQW-VCSEL. The high speed switching operation offered by a MQW laser over a bulk laser is clearly shown in Fig. 4b.

The dependence of transient response on the parameters of the VCSEL structure is also investigated. The turn-on delay time t_d, and the overshoot power P_v are used to describe the dynamic behavior of the MQW laser. The time t_d indicates that stimulated emission dose not occur until the carrier density has reached its threshold value N_{th}. Figures (5a, and 5b) display, respectively, the dependence of t_d on the facet reflectivity R and the number of wells N_w. The broken lines in these figures are related to the bulk laser. Figure (5a) highlights strongly the difference between t_d level for MQW and bulk laser. Also, the figure reveals that reduction of t_d can be obtained by increasing the facet reflectivity. This result can be explained by noting increasing R will reduce the total cavity loss and hence yields a reduction in the threshold carrier density required for stimulated emission. The time t_d increases smoothly with the increase of N_w since linear dependence exists between the volume of active region and N_w.

The variation of P_v with R and N_w is depicted in Figs.6a and 6b, respectively. Results for both MQW and bulk VCSELs are included for purposes of comparison. Investigation of these figures highlights the following findings:

(i) For MQW laser, P_v is a decreasing function with R, while P_v peaks at R=0.99 for bulk laser.

(ii) Increasing the number of wells employed in active region will increase the level of P_v monolithically. This effect arises from the linear dependence of volume V on N_w.

V -Conclusion

The transient response of MQW – VCSELs has been investigated using single- mode rate equations and taking account an accurate model to assess the dependence of the optical gain coefficient of the MQW active region on carrier density and structure parameters. The sensitivity of switching characteristics due to various structure parameters is addressed

Table I: Definition of Parameters

Definition	Symbols
Current	I(A)
Number of well	N_w
Electron charge	q
Optical confinement factor	Γ
Group velocity	V_g (cm/sec.)
Lasing photon energy	$E_{ph} = \hbar\varpi\,(eV)$
Angular frequency	ϖ
Nonradiative recombination coefficient	A_{nr} (s^{-1})
Auger recombination coefficient	C($1/s.cm^{-6}$)
Total cavity losses	γ (cm^{-1})
Active region scattering	γ_{ac} (cm^{-1})
External regions scattering	γ_{ex} (cm^{-1})
Mirror losses	γ_m (cm^{-1})
Top mirror reflectivity	R_t
Bottom mirror reflectivity	R_b
Effective cavity length	L_t(nm)
Geometrical mean of the mirror reflectivity	$R = \sqrt{R_b R_t}$
Well thickness	W_z(nm)
Barrier thickness	W_b(nm)
Cladding thickness	W_c(nm)
Penetration depth of the distributed facet mirror	W_m(nm)
Spontaneous emission rate	$\beta(cm^{-3})$
Laser wavelength	λ (μm)
Spontaneous emission spectral width	$\Delta\lambda_{sp}$ (nm)
Group refractive index	μ
Gain compression factor	ε (cm^{-3})

Table II: Parameter values of 1.3 μm In0.47 Ga0.53 As-In P MQW-VCSEL used in the simulation

Symbols	Value
W_z	4.3 nm
W_b	10 nm
W_c	1μm
N_w	12
E_g	751.8 meV
ΔE_c	$0.4E_g$
ΔE_v	$0.6E_g$
Δ	371.8 meV
m_c	$0.04368\ m_o$
m_H	$0.447\ m_o$
m_L	$0.03064\ m_o$
m_{c1}	$0.08\ m_o$
m_{H1}	$0.45\ m_o$
m_{L1}	$0.12\ m_o$
τ_{in}	0.1 ps
μ_a	3.5
R	0.9
$\Delta\lambda_{sp}$	60 nm
μ	3.2
A_{nr}	10^8 s
C	$3x10^{-24}$ cm^6/s
ε	10^{-17} cm^3
I_o	0 mA
P_o	3 mW

Table III: Subbands and their populations

n	*Quantized Energy (meV)*	*Population of the band**
Conduction Band		
0	158.802	1.0
Heavy Hole Band		
0	30.19	0.9637
1	118.491	0.0360
2	294.761	0.0002
Light Hole Band		
0	298.884	0.0001

* *The populations are normalized to $3x10^{18}$ cm^{-3}.*

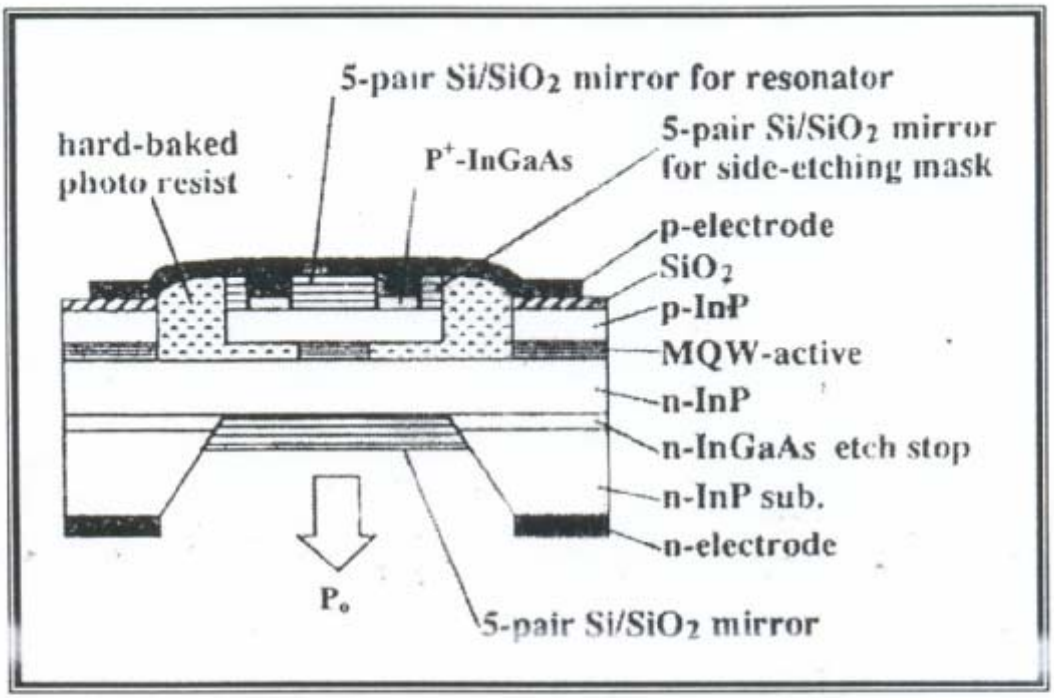

a

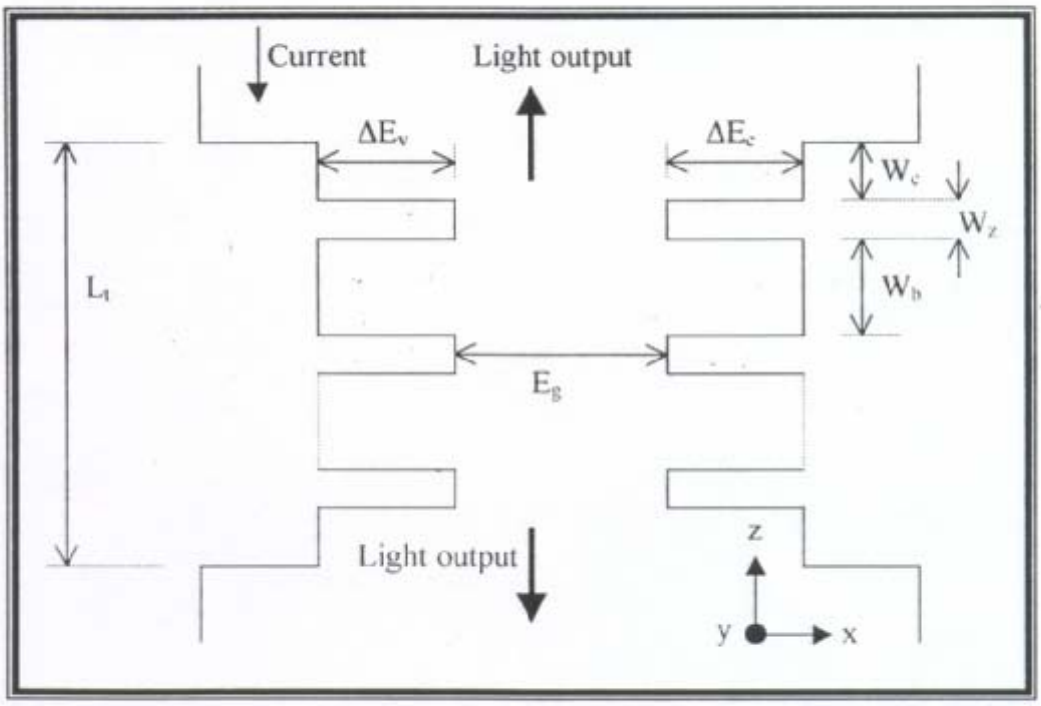

b

Fig. 1: a- Schematic cross section of the 1.3 µm MQW-VCSEL.
b- The potential profile of InGaAs/InP MQW laser.

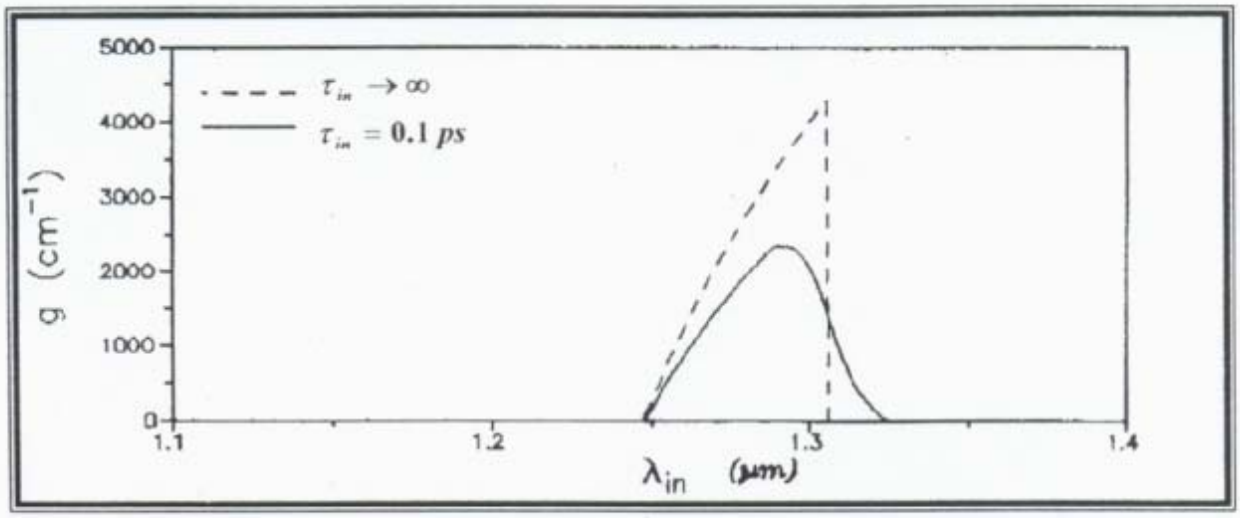

Fig. 2: Gain spectra of MQW-VCSEL for different value of τ_{in}.

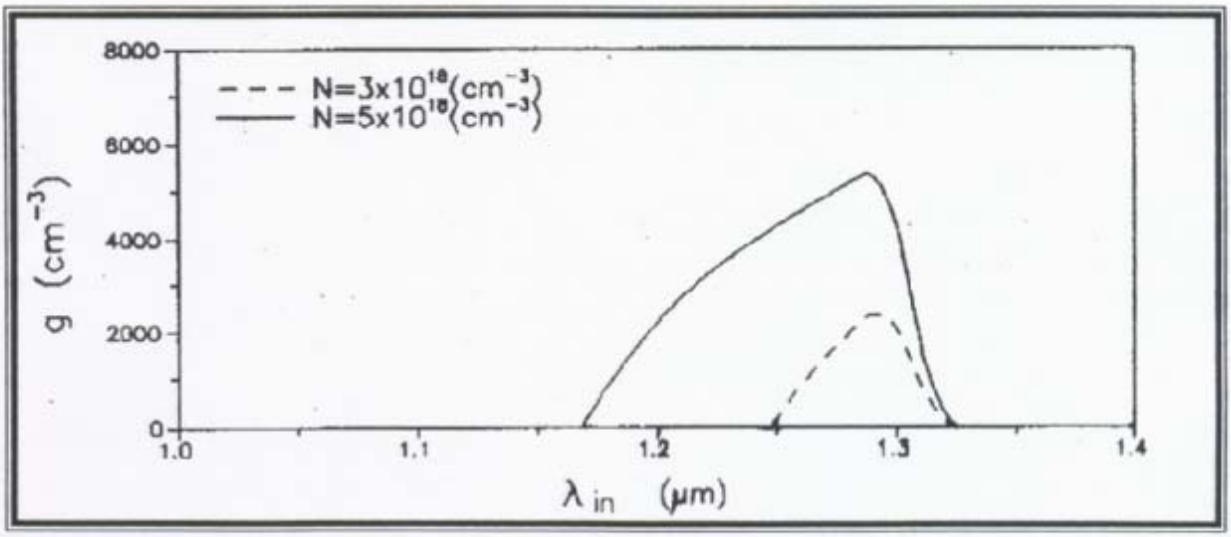

Fig. 3: Gain spectra of MQW-VCSEL for different value of N.

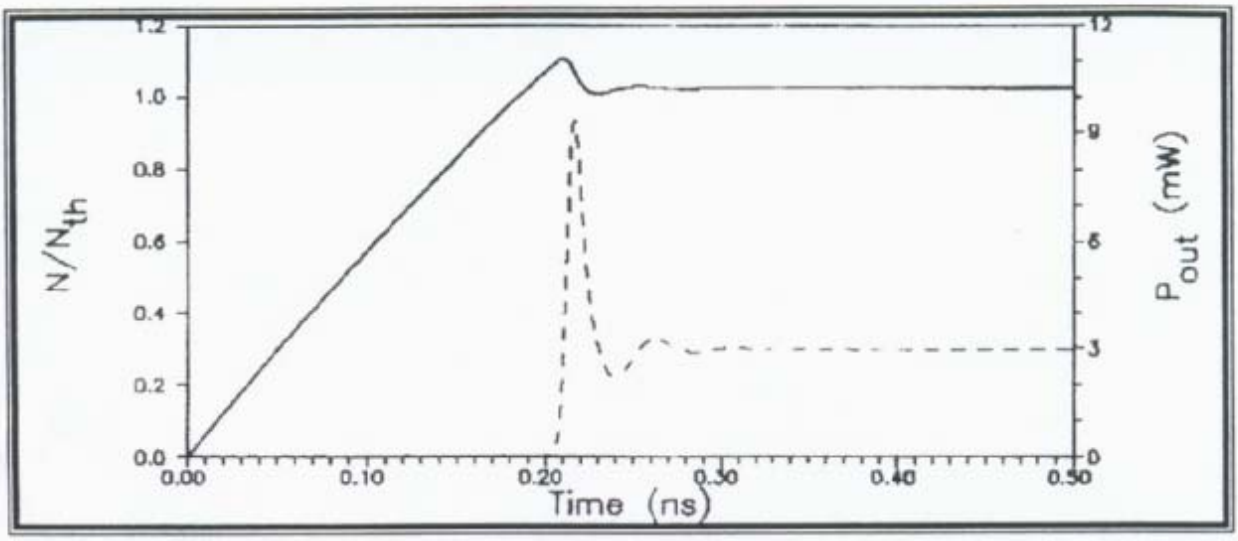

a

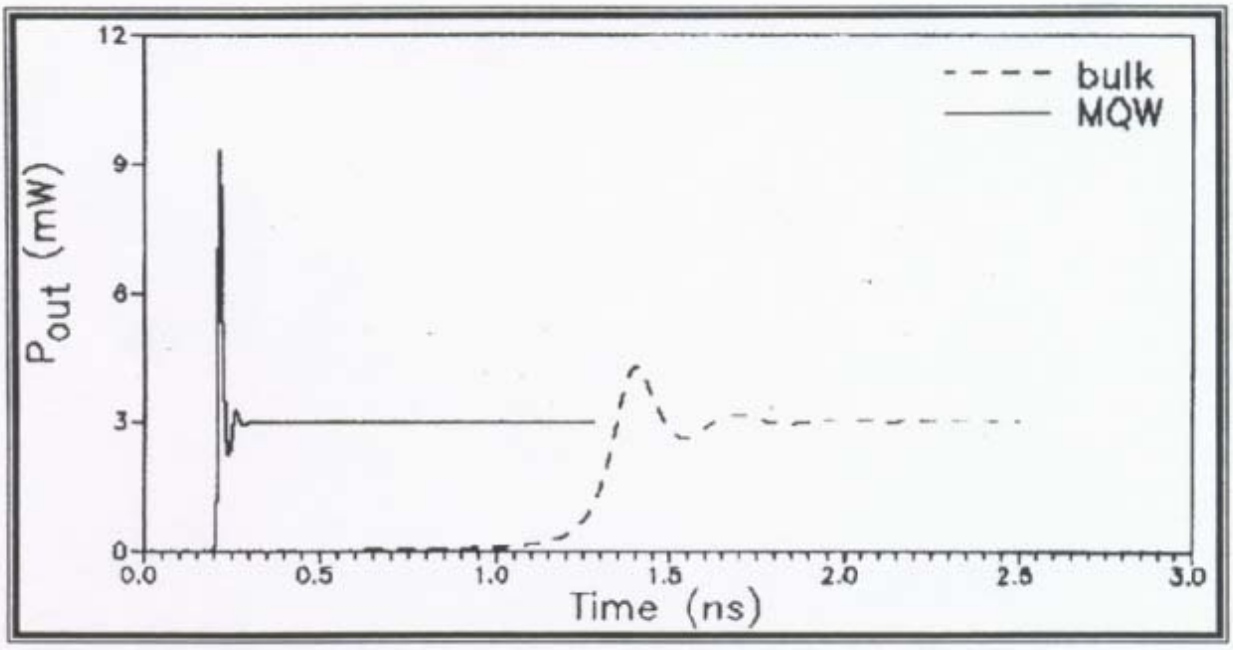

b

Fig. 4: a- Transit response of normalized carrier population and output power given by, respectively, solid curve and dashed curve.
b- Transit response of output power for MQW and bulk VCSEL.

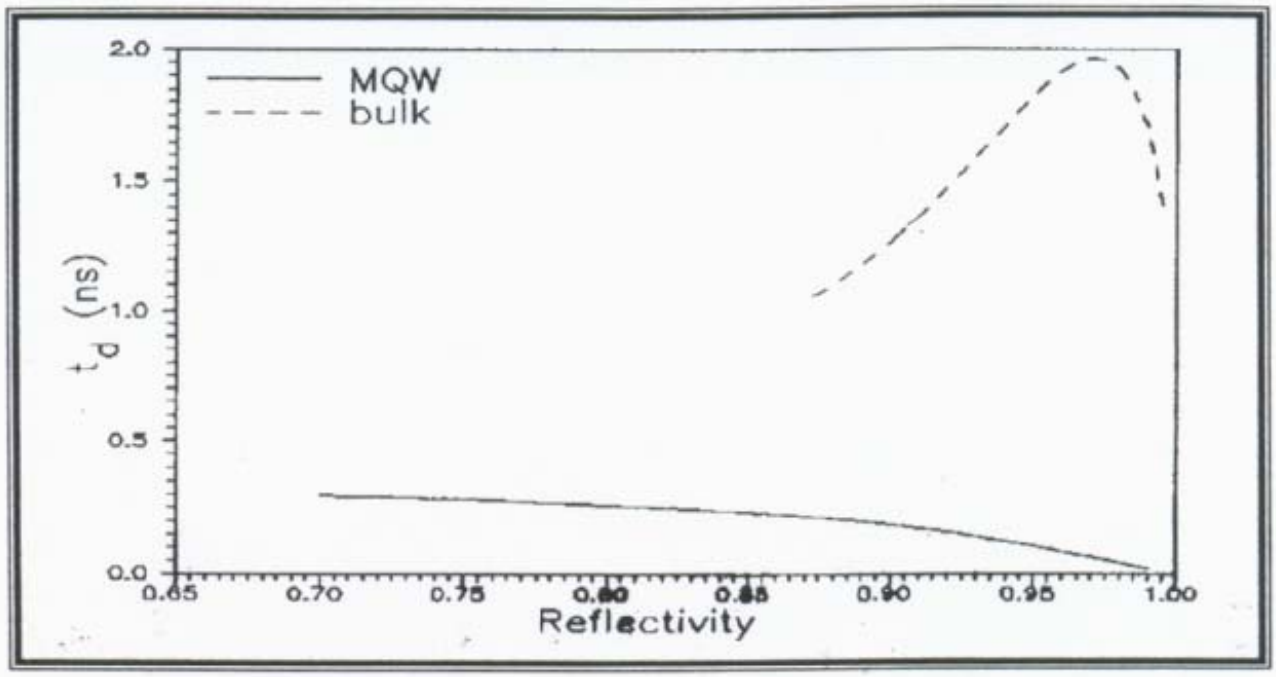

a

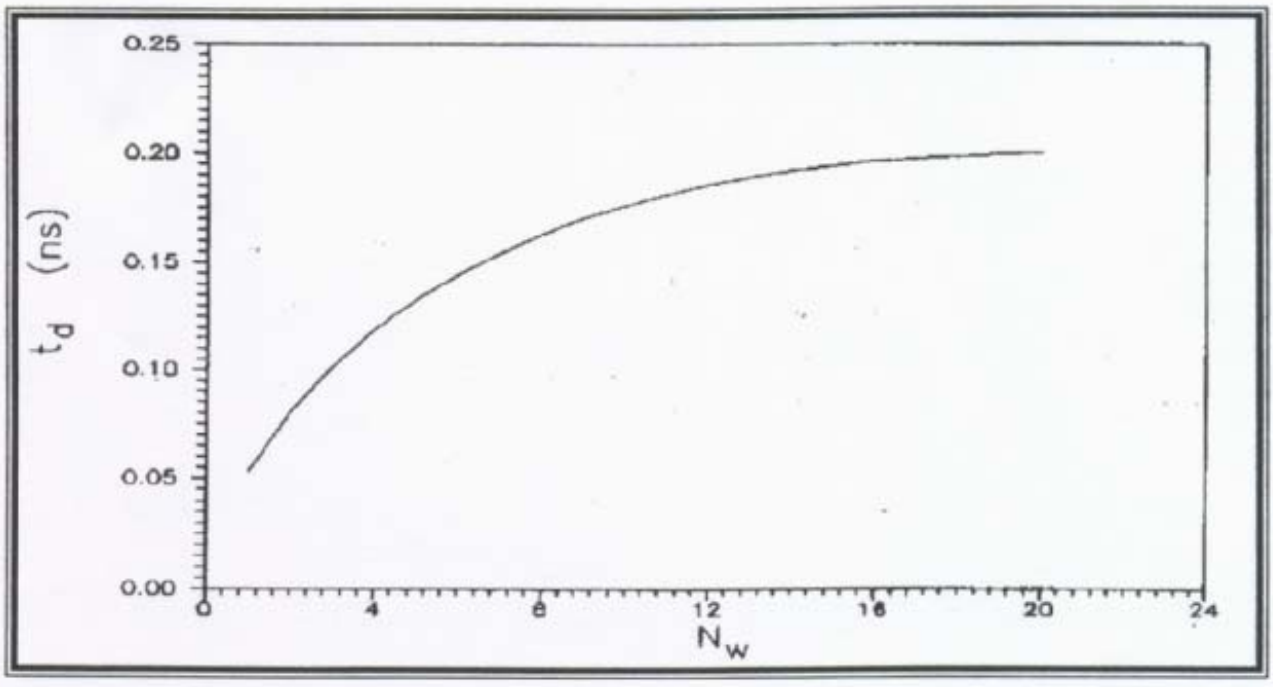

b

Fig. 5: Variation of turn-on delay time t_d with:
a- Reflectivity.
b- Number of wells.

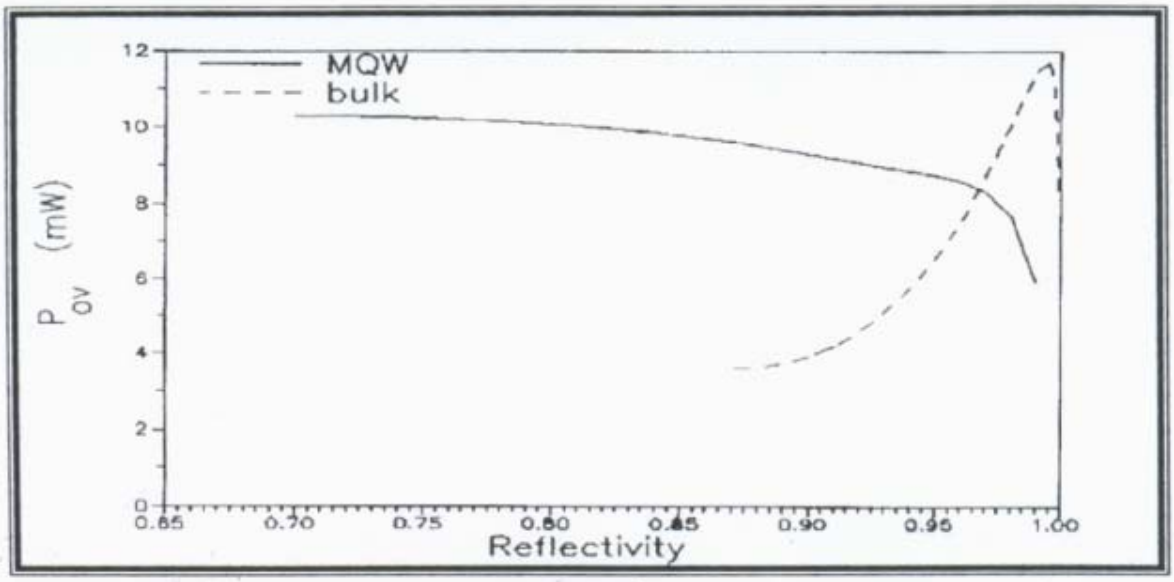

a

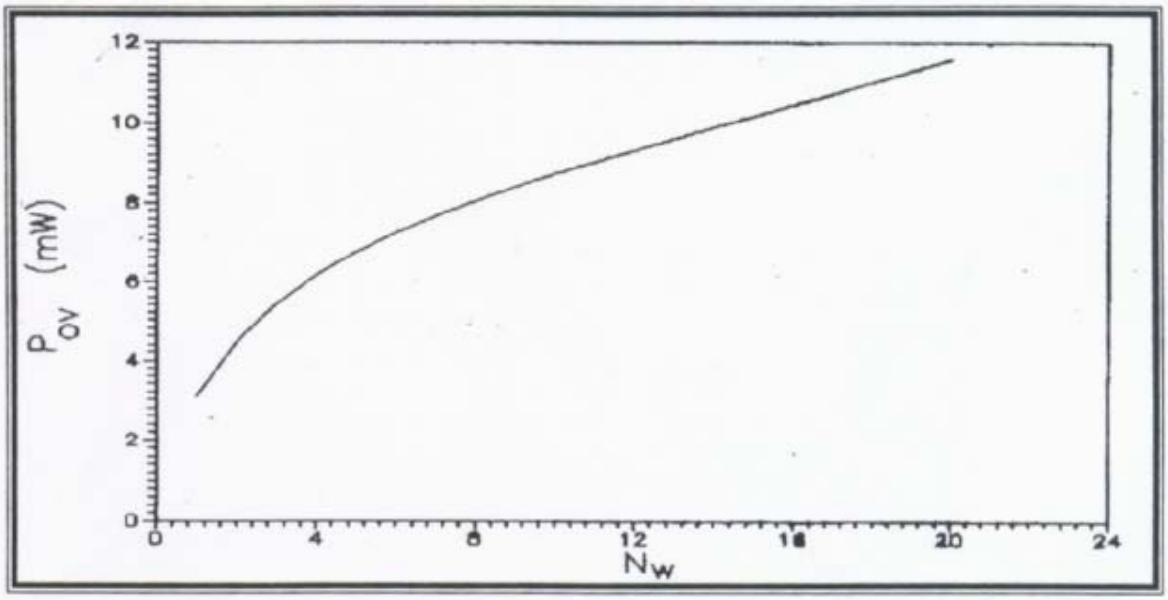

b

Fig. 6: Variation of overshoot power P_v with:
a- Reflectivity.
b- Number of wells.